THE AMERICAN SOCIETY OF MECHANICAL ENGINEERS
345 E. 47 St., New York, N.Y. 10017

92-GT-180

Behaviors of the Laterally Injected Jet in Film Cooling: Measurements of Surface Temperature and Velocity/ Temperature Field Within the Jet

SHINJI HONAMI and TAKAAKI SHIZAWA

Mech. Engineering Dept.
Science University of Tokyo
Kagurazaka, Shinjuku, Tokyo 162, Japan

ATSUSHI UCHIYAMA
Takasago Machinery Works
Mitsubishi Heavy Industries Ltd.
Takasago, Hyogo 676, Japan

ABSTRACT

This paper presents the behaviors of the injected jet on the flat surface in lateral injection of the film-cooling. Simultaneous velocity and temperature measurements were made by the double-wire probe. The test surface was also covered with an encapsulated temperature-sensitive liquid crystal. The image processing system based on the temperature and hue of the liquid crystal calibration provides the surface temperature distributions. The tests were conducted at three kinds of mass flux ratio of 0.5, 0.85, and 1.2. The laterally injected jet has an asymmetric structure with a large scale of vortex motion in one side caused by the interaction with the primary stream. Asymmetry is promoted with mass flux ratio increased, resulting in low film-cooling effectiveness.

NOMENCLATURES

D	Injection hole diameter
I	Momentum flux ratio($= \rho_2 U_2^2 / \rho_\infty U_\infty^2$)
M	Mass flux ratio($= \rho_2 U_2 / \rho_\infty U_\infty$)
T	Time-averaged temperature
U	Time-averaged velocity
X,Y,Z	Coordinate, see Fig. 1(a)
ϕ	Injection angle to streamwise direction
θ	Non-dimensional temperature($=(T - T_\infty)/(T_2 - T_\infty)$)

Subscript

∞	primary stream
2	secondary injected jet
w	surface

INTRODUCTION

The constant effort to increase the turbine inlet temperature has been made in the last decades. Film cooling is one of techniques which may satisfy the requirements for the thermal protection of the exposed turbine blade from hot combustion gases. Although a large number of experimental works on film cooling has been undertaken to provide the design data, recent emphasis is placed on a more detailed work on the jet behavior or a combined effect of the individual parameters by Sinha et al.(1991) and Honami & Fukagawa(1987). The interaction of the vortex generator and the injected jet through a single hole was investigated in the application of the film-cooling by Ligrani et al.(1991). Even though there has been a lack of understanding of the behavior of the laterally injected jet, Compton and Johnston(1991) studied the fluid dynamics behaviors of the jet from a single hole from the view point of the control or suppression of turbulent boundary layer separation by a vortex generator jet. Discrete-hole injection offers some complexity such as the three dimensional nature on the fluid dynamics and heat transfer behaviors. As most of the studies have been made individually on the surface heat transfer or the fluid dynamics behaviors of the injected fluid in lateral injection, there has been no detailed study dealing with the integrated results of the individual aspects.

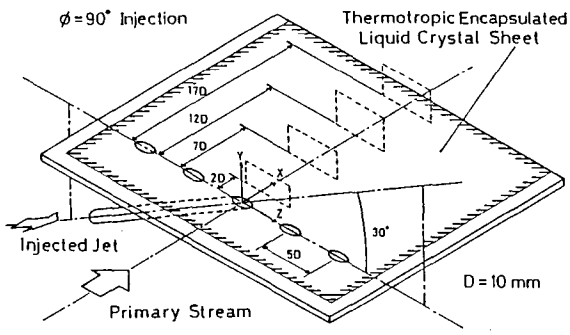

Fig. 1(a) Experimental apparatus (dimensions in mm)

Presented at the International Gas Turbine and Aeroengine Congress and Exposition
Cologne, Germany June 1-4, 1992
This paper has been accepted for publication in the Transactions of the ASME
Discussion of it will be accepted at ASME Headquarters until September 30, 1992

Table 1 Experimental Condition

Mass Flux Ratio	Density Ratio	Momentum Flux Ratio
0.50	0.85	0.294
	0.95	0.263
0.85	0.85	0.850
	0.95	0.761
1.20	0.85	1.694
	0.95	1.516

The objective of the present research is to obtain understanding of the injected jet behavior and its film-cooling effectiveness in lateral injection with mass flux ratio varied. The present paper provides detailed data both velocity/temperature fields within the injected jet and temperature field on the surface in lateral (spanwise) injection from a row of the holes. Emphasis is placed on the measurement of the velocity/temperature fields in the jet by using a double-wire probe, i.e., a constant temperature type of a hot-wire anemometer and a constant current type of a thermo-resistance meter. Another measurement also focuses on the temperature fields on the surface,i.e., film-cooling effectiveness from the image processing of temperature sensitive liquid crystal. The results obtained for the three mass flux ratios of 0.5, 0.85 and 1.2 will be discussed.

EXPERIMENTAL APPARATUS AND TECHNIQUES

Fig. 1(a) shows a schematic of the experimental test rig. A two dimensional 10:1 contraction nozzle is followed by a flat surface test section of 900 mm in length, 600 mm in width, and 100 mm in height. The tripping wire was installed at the inlet of the flat surface to provide a turbulent boundary layer over the test region.

Fig. 1(b) shows a cross section of an injection hole looking downstream direction. Five holes in a row which are spaced five hole-diameters apart are located 430 mm downstream of the trip. The hole pitch of five was selected, since wide spread of the injectant is expected in lateral injection. A row of injection holes having a diameter of 10 mm is arranged at a pitching angle of 30 degrees to the surface and an injection angle of 90 degrees to streamwise direction. The secondary air is injected at a higher temperature than the primary stream as in many studies of film cooling. The injected air is heated through the brass tube

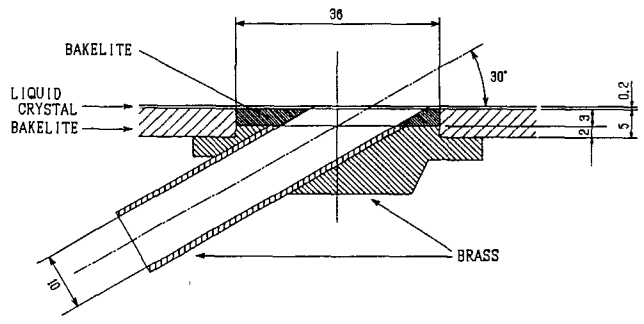

Fig. 1(b) Cross section of injection hole

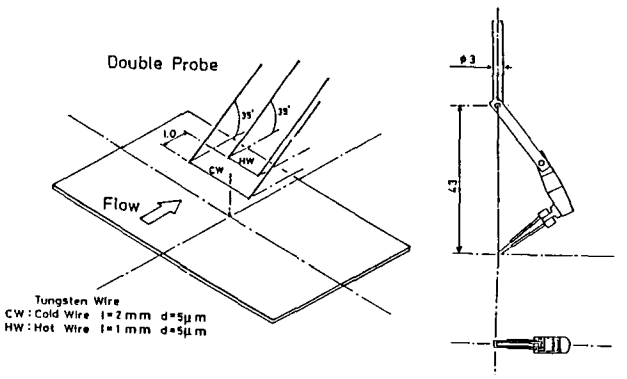

Fig. 2 Double-wire probe

wrapped with a ribbon type of the nickel-chrome heater and insulator.

Fig. 2 shows a double-wire probe. It provides with the simultaneous velocity and temperature measurements by a constant temperature type of a hot-wire anemometer with a tungsten wire of 5μm in diameter and 1 mm in length and a constant current type of a thermo-resistance meter with a tungsten wire of 5μm in diameter and 2 mm in length. The temperature compensation of the hot-wire was made by an output voltage of the thermo-resistance meter. The injected air temperature was maintained 55 K above the primary stream one.

Fig. 3 shows an image processing system by taking the image of the thermotropic liquid crystal by a black and white CCD camera. The test surface was covered with a thin sheet of encapsulated temperature-sensitive liquid crystal to visualize the surface temperature fields. The individual image data of three principal colors were taken through the camera with three kinds of optical filter resolved into red, green, and blue color. The hue is obtained through the reduction process of the above data of which noise is eliminated by a spatial filter by using an image processor and a personal computer. The image processor with the high resolution of 512 by 512 pixels and the intensity resolution of 8 bits was employed. The hue and temperature calibration for the liquid crystal was conducted at the outlet of the calibration wind tunnel in which an air-temperature can be controlled by a heater. The temperature of the injected air is 18 K above the fluid temperature of the primary stream because of the limitation of measurable range of the liquid crystal.

All the test were conducted in the primary air with the free-stream velocity of 13.5 m/s. The momentum thickness Reynolds number at the test section is 1100. The ratio of displacement thickness to the injection hole diameter is 0.18-0.20 at the test section. Table 1 shows the test condition of the secondary injected air and the primary stream. The density ratio is kept constant at 0.85 for the double-wire measurement and at 0.95 for the liquid crystal one.

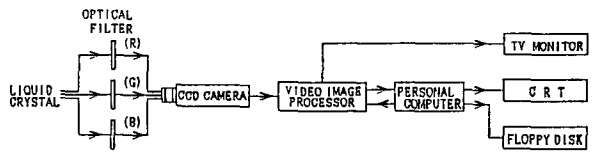

Fig. 3 Image processing system

RESULTS AND DISCUSSIONS

Temperature Profiles in the Jet

Fig. 4 shows contours of the non-dimensional time-averaged temperature measured by the double-wire probe for different mass flux ratio. The injection hole center is located at Z=0 in the figure. An arrow indicates the injected jet orientation at the hole. The pattern of isotherms shows asymmetry with respect to the jet center in lateral injection. The primary stream with low temperature penetrates into the bottom of the jet in the left side of the injected jet looking downstream, whereas no penetration of the low temperature fluid occurs in the right side.

Such asymmetry is maintained in the downstream direction. The peak temperature in the jet center decreases rapidly near the injeciton hole and more slowly in the farther downstream region. For higher mass flux ratio, the injected jet lifts up into the primary stream. The primary stream penetrates deeply into the left side of the jet and the jet bottom in the right side still remains near the surface. As to the high temperature region in the jet center among the different mass flux ratio near the injection hole, it is located near the surface for low mass flux ratio, but far from the surface for higher mass flux ratio. In particular, it is observed in the upper left side at mass flux ratio of 1.2.

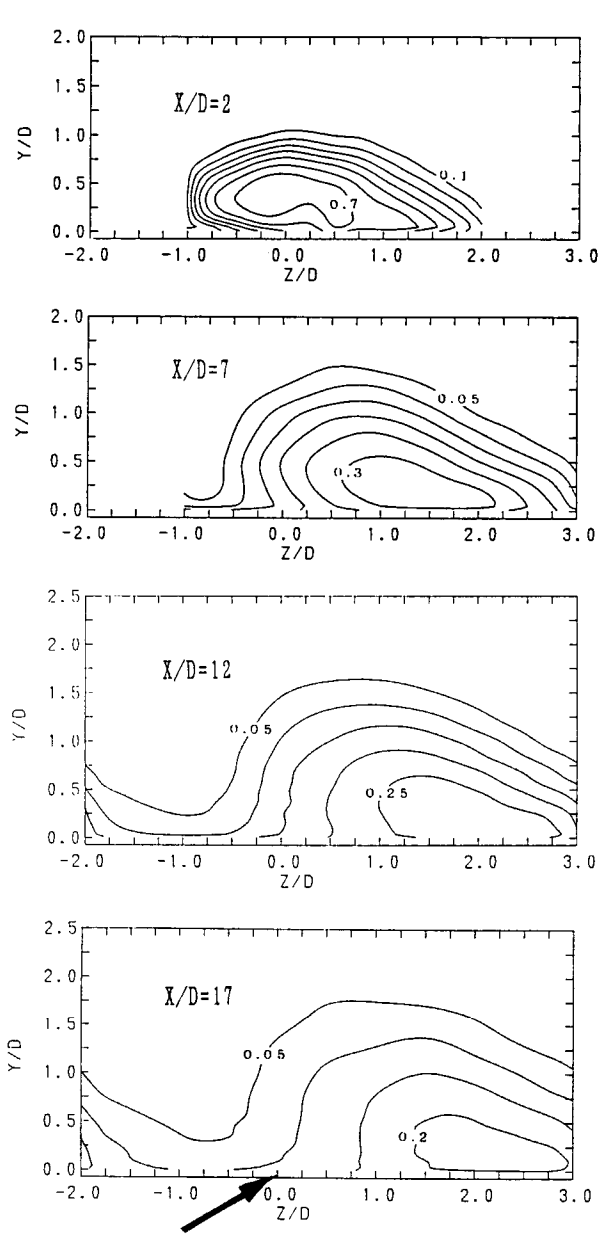

(a) M = 0.50

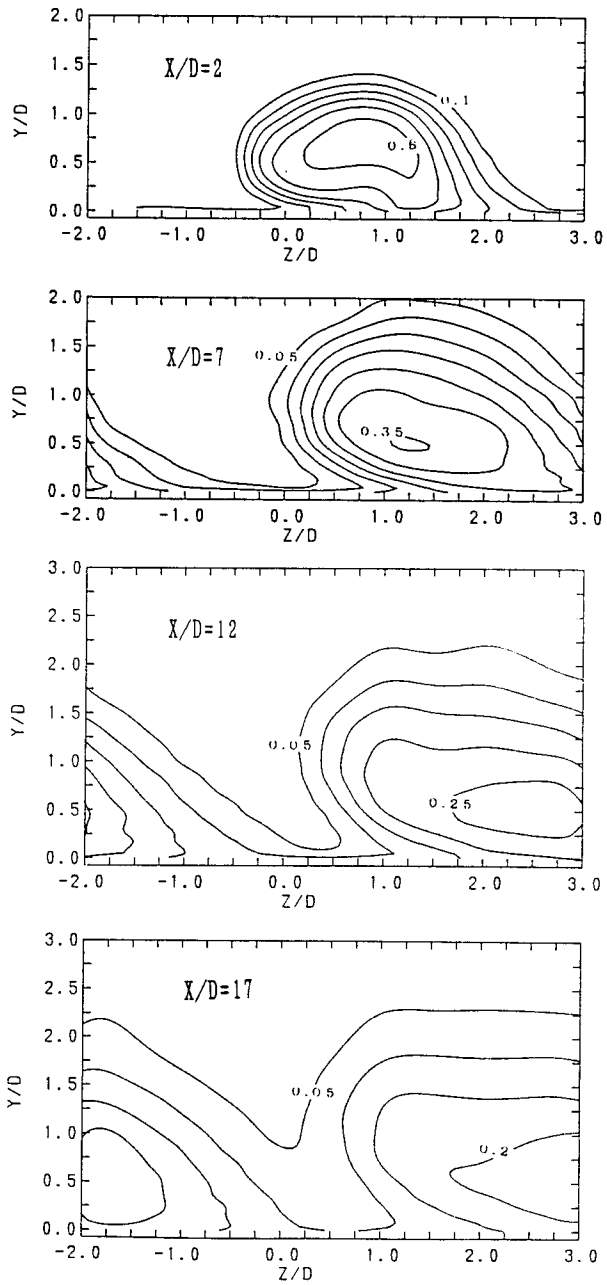

(b) M = 0.85

Fig. 4 Time-averaged temperature contours, θ

Velocity Profiles in the Jet

Fig. 5 shows the time-averaged velocity contours, U/U_∞. The data at X/D=2 were discarded, since the injected jet was forced to change from lateral to streamwise direction of the flow by the primary stream near the hole, and then the single hot-wire was not suitable for the measurement in the highly three dimensional flow field with high turbulence intensity. The profiles show asymmetry with respect to the jet center as in the temperature profiles, although asymmetry was not so clear as the temperature ones for low mass flux ratio. The local, high velocity region is observed around the jet, because the primary stream is accelerated by getting over the injected jet. At the farther downstream station, boundary layer becomes thin in the left side of the jet. As the mass flux ratio is increased, the local acceleration of the primary stream and the thinning of the boundary layer are promoted. The injected jet shows the isolated contours which corresponds to the jet center, since the location of the locally low velocity region coincides with that of the locally high temperature region, i.e., the jet center.

Compton and Johnston(1991) obtained velocity vector and velocity contours in the experiments of the vortex generator jet, as shown in Fig. 6. Their experiment is almost the same as the present one, except the pitching angle of 45 degrees and the hole diameter of 6.35 mm. They observed a clear vortex motion in the laterally injected jet at the velocity ratio of 1.0, which corresponds to mass flux ratio of 0.85 in the present experimental condition, density ratio being 0.85. They also found that the maximum vorticity became large with increasing the velocity ratio, VR, from 0.7 to 1.3. The jet boundary indicated asymmetry like the present injected jet. The maximum vorticity levels were strongly dependent on the velocity ratio, VR, and a skew angle which was the injection angle in the present paper. An optimal skew angle which might offer the best

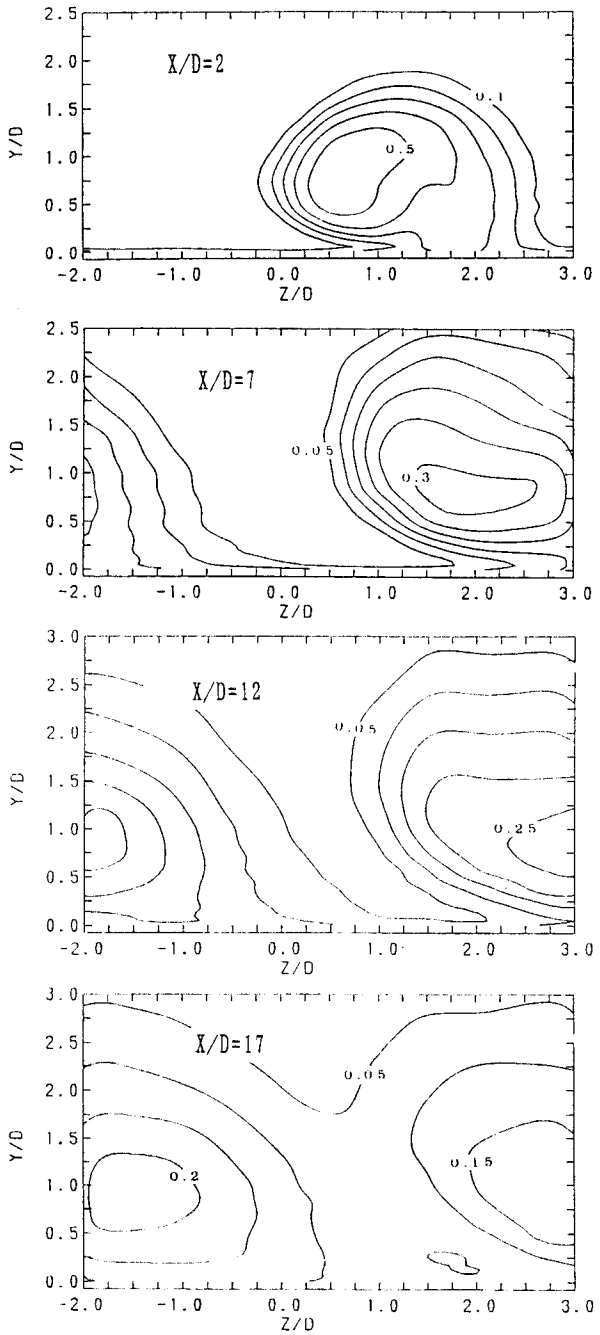

(c) M = 1.2

Fig. 4 Time-averaged temperature contours, θ

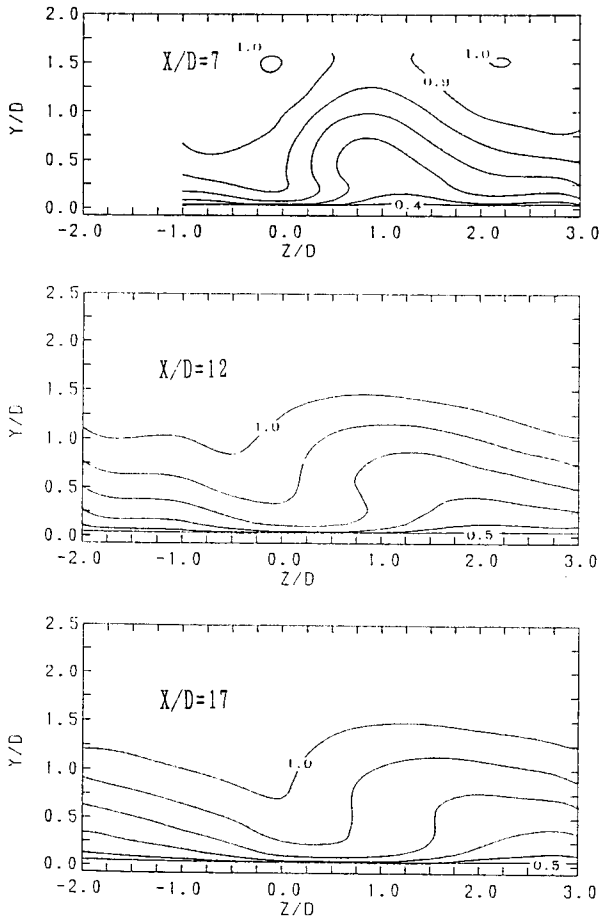

(a) M = 0.50

Fig. 5 Time-averaged velocity contours, U/U_∞

performance in suppression of separation, in other words, the strong vortex motion, might be between 45 and 90 degrees.

As a result, a large scale of one vortex motion was confirmed in the laterally injected jet by Compton's experiment. It is shown through comparison with their result that the jet behavior is dependent on the vortex intensity induced by the primary stream, i.e., the vorticity in the jet. Hence, the primary stream promotes the vortex motion in the left side of the jet and suppresses it in the right side. This vortex motion causes the injected jet to detach from the surface with mass flux ratio increased.

Surface Temperature Profiles

Fig. 7 shows the temperature contours on the surface of the test section in lateral injection. The non-dimensional surface temperature corresponds to film cooling effectiveness, since the definition is the same as each other. The direction of the injection is in the positive spanwise z-direction. The broad band of the temperature contours of 0.2 is observed due to the calibration of the liquid crystal in which the curve has a weak sensitivity to temperature in this temperature range. The high temperature region is located in the positive spanwise direction as the mass flux ratio becomes large. The injected jet for mass flux ratio of 0.5 covers the wide region of higher temperature, while the low temperature region is obtained for the high mass flux ratio of 1.2.

The locally low temperature region is observed near the injection hole, i.e., X/D=1 and Z/D=-1, even though effect of the thermal conductivity near the injection hole is considered because of the thinner insulator than that of the test surface, as shown in Fig. 1(b). This feature becomes more marked with increasing the mass flux ratio. The sharp kink of isotherms of θ=0.35 for mass flux ratio of 0.5, and θ=0.30 for mass flux ratio of 0.85 and 1.2 are shown in the figures.

Injected Jet Behaviors

Fig. 8 shows the combined temperature fields obtained from the measurements by the double-wire probe and the liquid crystal. The near surface temperature in

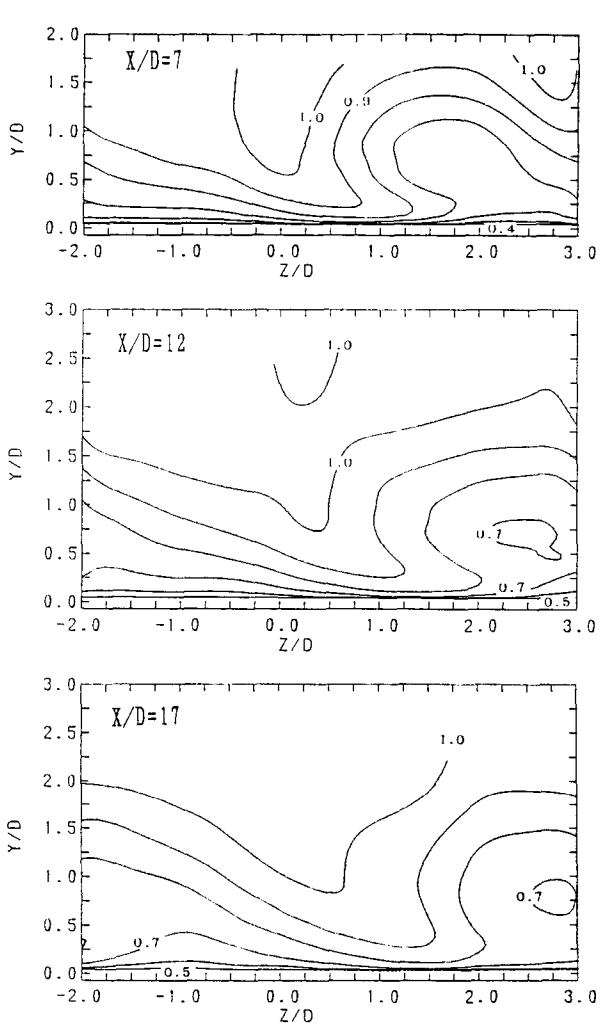

(b) M = 0.85

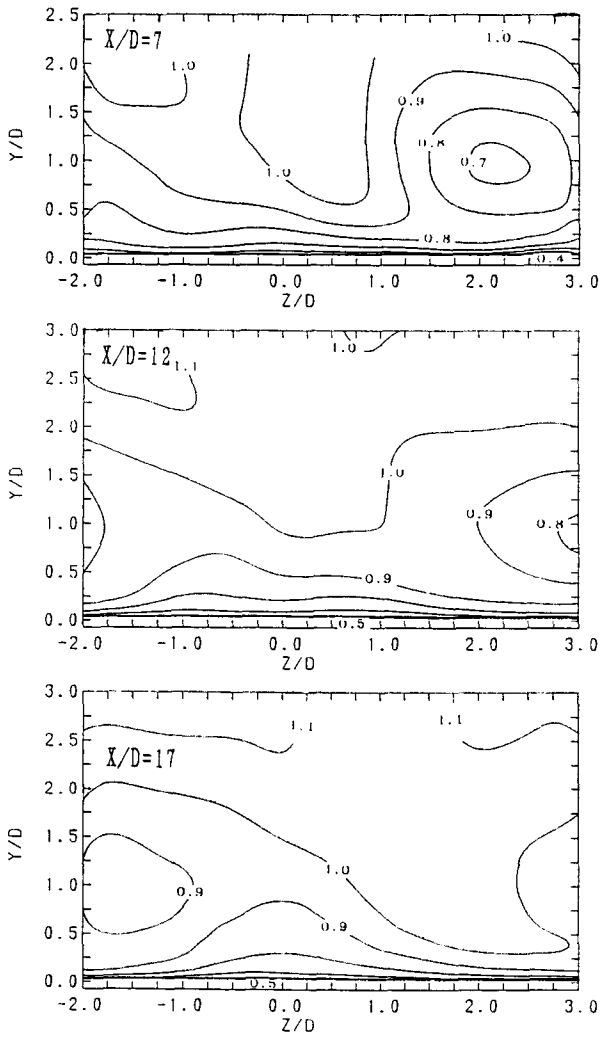

(c) M = 1.2

Fig. 5 Time-averaged velocity contours, U/U_∞

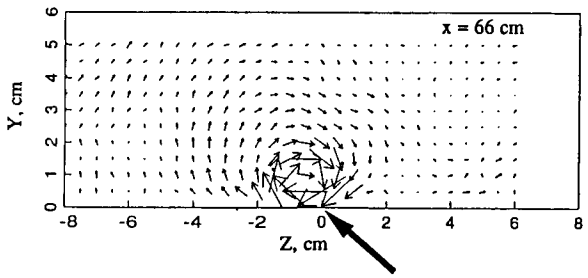

(a) Secondary velocity vectors for VR=1.0. Large arrow indicates jet orientation.

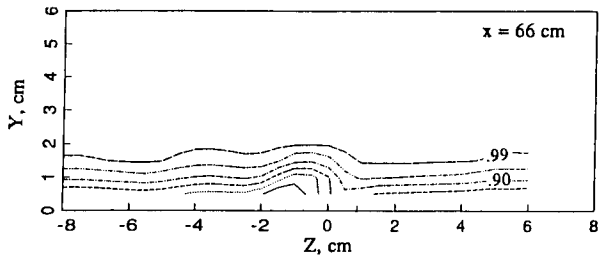

(b) U/U_∞ contours. Intervals are by 0.05, except the final contour, which is located at boundary layer edge.

Fig. 6 Experiment of vortex generator jet from Fig. 2 by Compton and Johnston(1991)

the injected jet measured by the probe corresponds to the surface temperature distribution by the liquid crystal. Maximum surface temperature shifts in the spanwise direction as the jet proceeds in the downstream direction. The spanwise location of the maximum temperature in the jet deviates from the geometric center of the jet with increasing mass flux ratio, because the rolling down of the primary stream results in the low surface temperature in the downwash region of the left side of the jet. But the high surface temperature is obtained in the right side due to the attached jet without the vortex motion. The exact behaviors of the injected jet could not be expected from only the measurement of the surface temperature field in lateral injection. Furthermore, the isothermal line near downstream of the hole shows a large kink as mentioned before. This is another evidence that the rolling down of the main stream beyond the injected jet occurs close to the injection hole. Such a behavior of the jet produces a local change in film-cooling effectiveness, and causes damage of the blade material near the hole because of unexpected thermal stress. It is worth denoting that the asymmetric feature of the laterally injected jet is easily understood by the combined results on the temperature measurements on the surface and within the injected jet.

Fig. 9 shows a sketch of the jet behavior and the interaction of the jet and the primary stream based on the results obtained from the above-mentioned measurements for low mass flux ratio. Goldstein et al.(1970) showed the flow field associated with a laterally inclined jet with a large scale of two vortices structure. The laterally injected jet observed by the present experiment has the asymmetric structure with a large scale of one vortex motion promoted by the primary stream in the left side of the jet. Question is

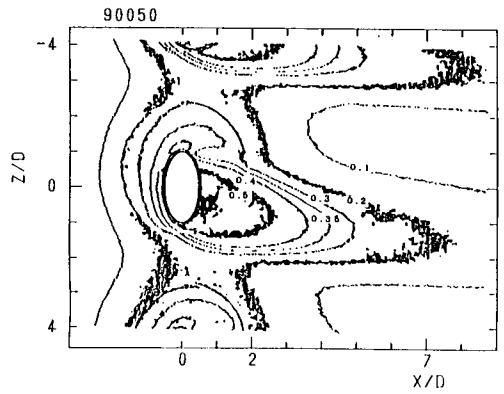

(a) M = 0.50

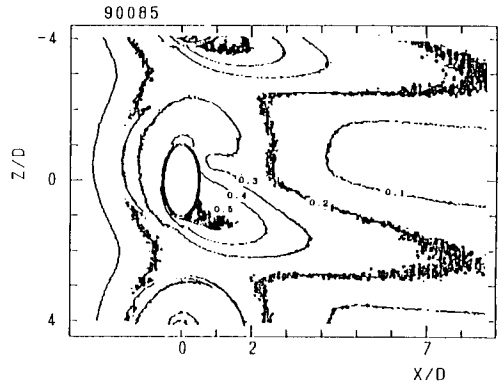

(b) M = 0.85

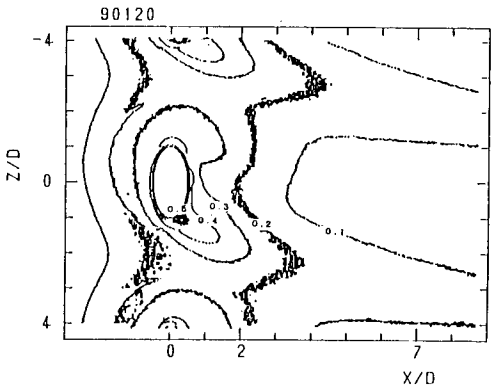

(c) M = 1.2

Fig. 7 Temperature contours on the surface

why the vortex motion cannot be observed in the right side as in stream-wise injection. It may be considered that a skewed boundary layer developes on the surface close to the hole because of strong streamline curvature of the jet, and then the vorticity in the skewed boundary layer is cancelled by the rolling up of the primary stream in the right side because of an opposite

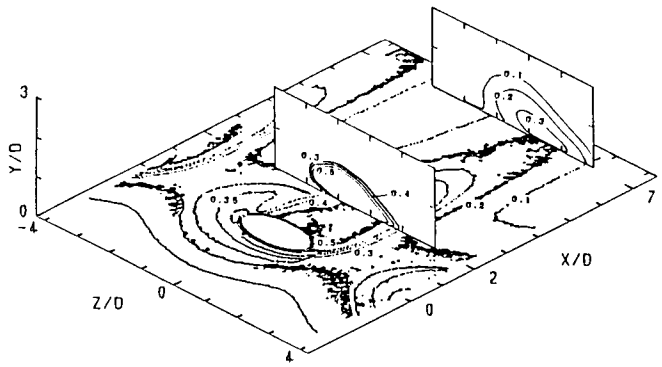

(a) M = 0.50

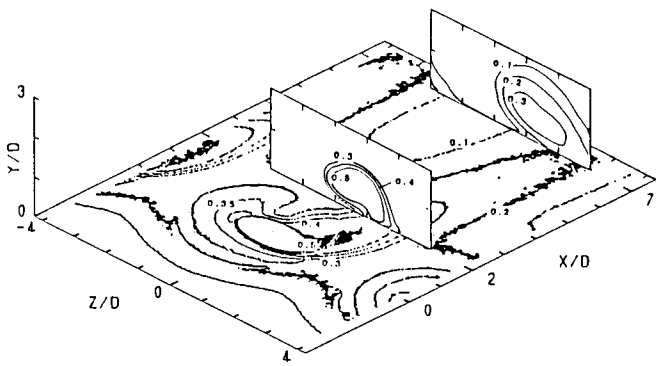

(b) M = 0.85

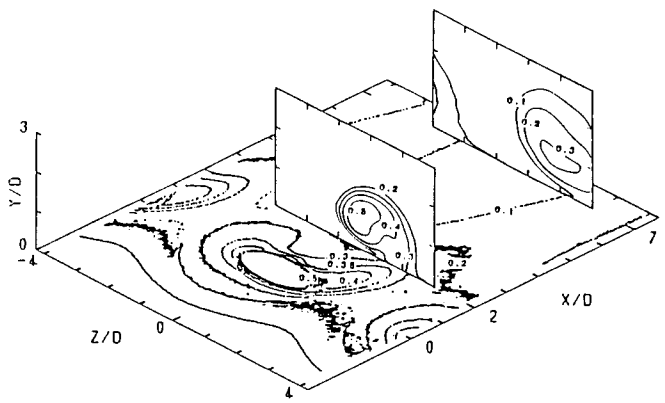

(c) M = 1.2

Fig. 8 Time-averaged temperature field

sign of the vorticity. Therefore, understanding of such features results in the improvements in film-cooling performance. The suppression of the vortex motion in the left side is a key technology to obtain higher film-cooling effectiveness, besides the wide spread of the jet in the spanwise direction with the mass flux ratio increased.

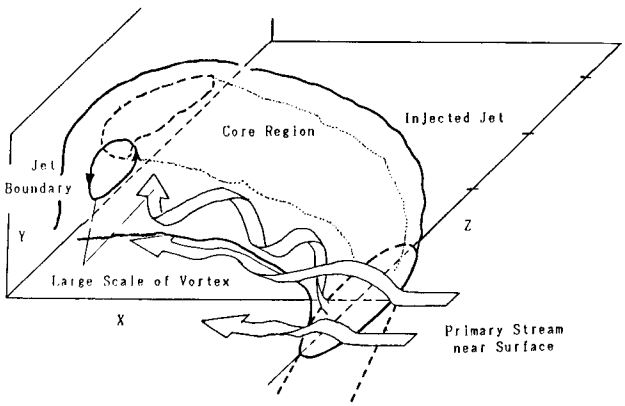

Fig. 9 Jet behavior in lateral injection for low mass flux ratio

CONCLUSIONS

Detailed measurements of the laterally injected jet on the velocity/temperature field by a hot-wire anemometer and a thermo-resistance meter and the surface temperature field by the temperature-sensitive liquid crystal were conducted. The following conclusions were obtained.

(1) The laterally injected jet has the asymmetric structure with a large scale of vortex motion promoted by the primary stream in one side of the jet, but suppressed in other side.

(2) There is a little contribution to the film-cooling in one side with the vortex motion, whereas the high film-cooling effectiveness is obtained in other side.

(3) The asymmetric structure in lateral injection is promoted with mass flux ratio increased, resulting in low film-cooling effectiveness.

ACKNOWLEDGEMENTS

We wish to thank Messrs. M. Kayama, H. Maseda, A. Namie, and M. Yamamoto who assisted in the data aquisitions. We also acknowledge the help of Mr. Y. Tanaka who constructed the data reduction system of the image processing.

REFERENCES

Compton, D. A. and Johnston, J. P.,1991,"Streamwise Vortex Production by Pitched and Skewed Jets in a Turbulent Boundary Layer," AIAA 91-0038.

Goldstein, R. J., Eckert, E. R. G., Eriksen, V. L. and Ramsey, J. W., 1970,"Film Cooling Following Injection through Inclined Circular Tubes," Israel Journal of Technology, Vol. 8, pp.145-154.

Honami, S. and Fukagawa, M., 1987,"A Study on Film Cooling - Behavior of a Cooling Jet over a Concave Surface," Proceedings of 1987 Tokyo International Gas Turbine Congress, Vol.3, pp.209-216.

Ligrani, P. M., Subramanian, C. S., Craig, D. W. & Kaisuwan, P., 1991,"Effects of Vortices with Different Circulations on Heat Transfer and Injectant downstream of a Single Film-Cooling Hole in a Turbulent Boundary Layer," ASME, Journal of Turbomachinery, Vol.113, pp.433-441.

Sinha, A. K., Bogard, D. G. & Crawford, M. E., 1991,"Film-Cooling Effectiveness Downstream of a Single Row of Holes with Variable Density Ratio," ASME, Journal of Turbomachinery, Vol.113, pp.441-449.